The American Journal of Human Genetics, Volume *99*

Supplemental Data

TBCE Mutations Cause Early-Onset Progressive Encephalopathy with Distal Spinal Muscular Atrophy

Antonella Sferra, Gilbert Baillat, Teresa Rizza, Sabina Barresi, Elisabetta Flex, Giorgio Tasca, Adele D'Amico, Emanuele Bellacchio, Andrea Ciolfi, Viviana Caputo, Serena Cecchetti, Annalaura Torella, Ginevra Zanni, Daria Diodato, Emanuela Piermarini, Marcello Niceta, Antonietta Coppola, Enrico Tedeschi, Diego Martinelli, Carlo Dionisi-Vici, Vincenzo Nigro, Bruno Dallapiccola, Claudia Compagnucci, Marco Tartaglia, Georg Haase, and Enrico Bertini

CASE REPORTS

Clinical features of the subjects included in the study are summarized below and are schematically listed in Table 1.

Subject 1544334. This subject, originating from the island of Ischia, Naples, was born on 2007 from first cousin parents, and was firstly examined at the age of 18 months because of delayed motor and cognitive development. At birth, weight was 3,240 g, and length was 50 cm. He was able to sit without support but was not able to walk, although moved in quadrupeds. Neurological examination documented signs of spasticity in his legs, and the brain MRI showed a thin corpus callosum with no additional abnormalities. The Griffith Mental Developmental scale scored 43 QG indicating moderate delay with ES -8.5 months. At 4 years, he was not able to walk, and could stand with support only for a short time because of spasticity, unsteadiness, and a bilateral foot drop. No fasciculations were detected. He was able to speak, using simple sentences, and had dysarthria. At 8 years, weight was 29 kg (50th-75th centile) and height was 125 cm (25th-50th centile).

Subject 2518864. This subject (b. 2009), also originating from the island of Ischia, was born from healthy and not related parents. Birth occurred when he was at the 38^{th} week of gestation (weight: 3,490 g; length: 35 cm; OFC: 35 cm). Hypotonia and poor antigravity movements were noticed during the first months of life, and severe developmental delay was noticed during the first year. The child was not able to control his head by age 10 months, and has never been able to sit. Neurological examination at 5 years showed an alert child who was not able to speak; he had limb weakness, which was more severe in lower limbs; sitting was possible with support. At 5 years, weight was 16 kg (25th centile), and height was 108 cm (50th centile). There was a bilateral foot drop, and bilateral foot clonus. Fasciculations were not detected. Swallowing was possible with difficulty.

Subjects 00997847 and 00997844. The two individuals (b. 2000) were monozygotic twins born from unrelated and healthy parents originating from Naples. Weight at birth (37 weeks of gestation without complications) was 3,030 and 2,570 g, respectively. The twin sibs had a clinical history of delayed milestones already in the first year of life. They achieved ability to sit alone at age 12 months, and were able to stand with support around age 18 months. At 2 years, they were able to speak in sentences but with severe dysarthria. The disease slowly progressed in both sibs, who manifested spasticity in their legs, ataxia, and distal amyotrophy of upper and lower limbs, without evidence of fasciculations. Both twins loosed autonomous sitting position by the age of 5 years. Around the age of 8 years, they started to have swallowing disturbances with drooling. Now, at 15 years, they are both wheelchair bond, showing severe distal amyotrophy of hands and feet, ataxia, spasticity, and scoliosis.

Subject VN_X3359. This young lady is the first child of healthy unrelated parents, both originating from the metropolitan area of Naples. She was born in 1996 after an uneventful pregnancy, and was

delivered at the 38th weeks of gestation by Caesarian section due to membrane disruption. Her birth weight was 2,060 g. Her developmental milestones were reported within normal epochs until the age of 12 months when she was noted to stand with difficulties. From the age of 14 months, developmental regression was observed together with progressive hypertonia of the four limbs. In the following months, distal amyotrophy and optic atrophy appeared. Moreover, she lost the ability to pronounce the few fords she had learned. At the age of 12 years, she also started suffering from frequent simple partial seizures. The patient came to our attention at the age of 18 years because of therapy resistant seizures. These were mainly characterized by focal hemiclonic convulsions, sometimes occurring in clusters. Neurological examination showed severe intellectual disability, absent language, spastic tetraparesis with distal amyotrophy, abnormal eyes movement, strabismus. The physical examination showed severe scoliosis.

Subject VN_X5360. This subject is the younger sibling of VN_X3359. He was born in 2001 after uneventful pregnancy, and was delivered at the 39th weeks of gestation with a birth weight of 3,250 g. His developmental milestones were reported normal until the age of 8 months when the child started exhibiting difficulties in holding his head and progressive hypertonia of the four limbs. Ataxia, dysarthria and optic atrophy subsequently appeared. He came under our attention at the age of 13 when he was wheelchair bound. At that time the neurological examination showed severe intellectual disability, dysarthria, spastic tetraparesis with distal amyotrophy, abnormal eye movements and strabismus. The physical examination showed severe scoliosis. He has never suffered from seizures; however the electroencephalography showed epileptiform abnormalities over the left parieto-occipital regions.

Additional laboratory investigations. Since inactivating mutations of *TBCE* had previously been documented to cause severe defects in calcium and phosphorus (Ca/P) metabolism and growth failure, extensive endocrinological and metabolic examinations were performed in all subjects. In 1544334, 2518864, 00997847 and 00997844, levels of Ca/P were within normal values. In 1544334, at 7 years, an extensive endocrinological investigation of the hypothalamic-pituitary-adrenal axis showed only a slightly reduced response to GHRF and reduced release of cortisol. Similarly, extensive endocrinological investigation in subjects 2518864, 00997847 and 00997844 yielded normal results. Importantly, no feature compatible with a diagnosis of hypoparathyroidism was documented; similarly, growth was normal in all individuals. Overall, the clinical phenotype in all subjects clearly differed from what observed in both hypoparthyroidism-retardation-dysmorphism (MIM 241410) and Kenny-Caffey syndrome (MIM 244460).

In subject 1544334, multimodal evoked potentials (VEPs) were normal. Motor nerve conduction velocity of lower limbs (45 m/sec in the right peroneal nerve) was normal with a markedly

reduced compound muscle action potential (CMAP) amplitude (0,5 mVs in the right extensor digitorum brevis muscle), while sensory conduction velocity and sensory action potential (SAP) of the sural nerve were normal (8 mVs, 48 m/sec), indicating a motor neuropathy. Similarly, in 2518864, multimodal electrophysiological examination showed normal brainstem evoked responses (BAERs), somatosensory evoked potentials (SSEPs) as well as sensory and motor nerve conduction velocities; CMAP had low amplitudes (0.4 mVs) in the extensor digitorum brevis of feet; visual evoked responses were slightly delayed with normal ERG. Electromyography (EMG) was performed in all subjects and showed clear neurogenic features in distal and proximal muscles of their legs characterized by polyphasic motor units, with increased duration, high amplitude, and recruitment with increased firing rate. Fibrillation potentials were detected only in distal muscles, while fasciculations were never detected. The muscle biopsy showed signs of denervation atrophy in subjects 1544334, 2518864, 00997847 and 00997844, the electrophysiological multimodal examination showed delayed VEPs, and BAERs, while SSEPs evoked from lower limbs were normal.

In all individuals, the ophthalmological evaluation documented bilateral optic atrophy. The brain MRI of subject 1544334 (2 years) showed a thin corpus callosum. A following MRI (3 years) showed a moderate global cerebellar atrophy and confirmed a thin corpus callosum. Subjects 2518864, 00997847 and 00997844 exhibited similar MRI features. In siblings VN_X3359 and VN_X5360, brain and spine MRIs performed at 17 (VN_X3359) and 13 (VN_X5360) years showed atrophy of the cerebellum, which was prominent in the vermis, and hypoplasia of the dorsal spine, together with white matter T2 hyperintensity in the posterior periventricular areas, T1 hypointensity areas in the pallidum and substantia nigra suggesting iron deposition, and marked corpus callosum hypoplasia. Similarly, in twin subjects 00997847 and 00997844, a MRI was performed at age 16 years and, besides showing atrophy of the cerebellum and marked corpus callosum hypoplasia, T2* relaxation weighted images confirmed that the hypointense T2 and FLAIR weighted areas corresponded to iron increase for age. In VN_X3359, electroencephalography showed bilateral epileptiform interictal abnormalities over the temporal lobes. Seizures were partially controlled under levetiracetam and phenobarbital.

Overall, these data confirm that all individuals suffer from progressive motor neuronopathy and spastic ataxia bearing similarities with the phenotype of the *pmn/pmn* mice. Surprisingly, follow-up MRIs performed in the second decade, particularly in VN_X3359 and VN_X5360, showed a pattern of neurodegeneration with brain iron accumulation (NBIA).

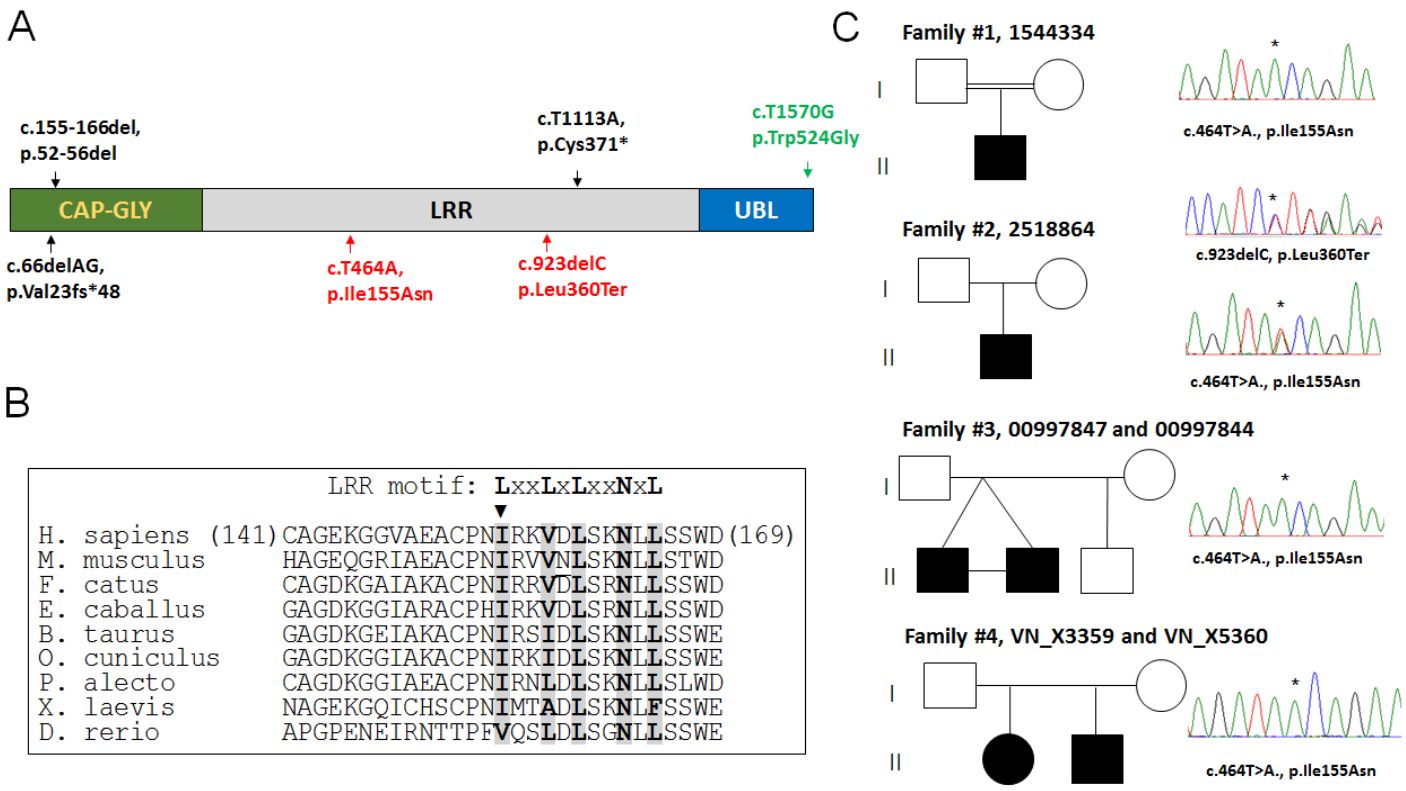

Figure S1. TBCE domain organization, *TBCE* mutations causing early-onset progressive encephalopathy with distal spinal muscular atrophy, and conservation of Ile^{155}.
(**A**) Schematic representation of TBCE and location of known disease-causing mutations. Mutations causing hypoparathyroidism-retardation-dysmorphism (HRD) and Kenny-Caffey syndrome (KCS) are shown in black, while those implicated in neurodegeneration are in red (present study) and green (*pmn*/*pmn* mouse).
(**B**) Multiple sequence alignment of TBCE orthologs. Ile^{155} is indicated (closed triangle). Columns corresponding to the consensus 'L/I' and 'N' residues in the LxxLxLxxNxL motif are highlighted in gray.
(**C**) Pedigrees of the 4 families and chromatograms of the relevant *TBCE* coding sequence showing the disease-associated mutation(s). The location of mutations are shown (asterisk) together with the nucleotide and amino acid changes. *TBCE* mutations are annotated according to the human sequence GenBank accession NM_001079515.2 and NP_001072983.1.

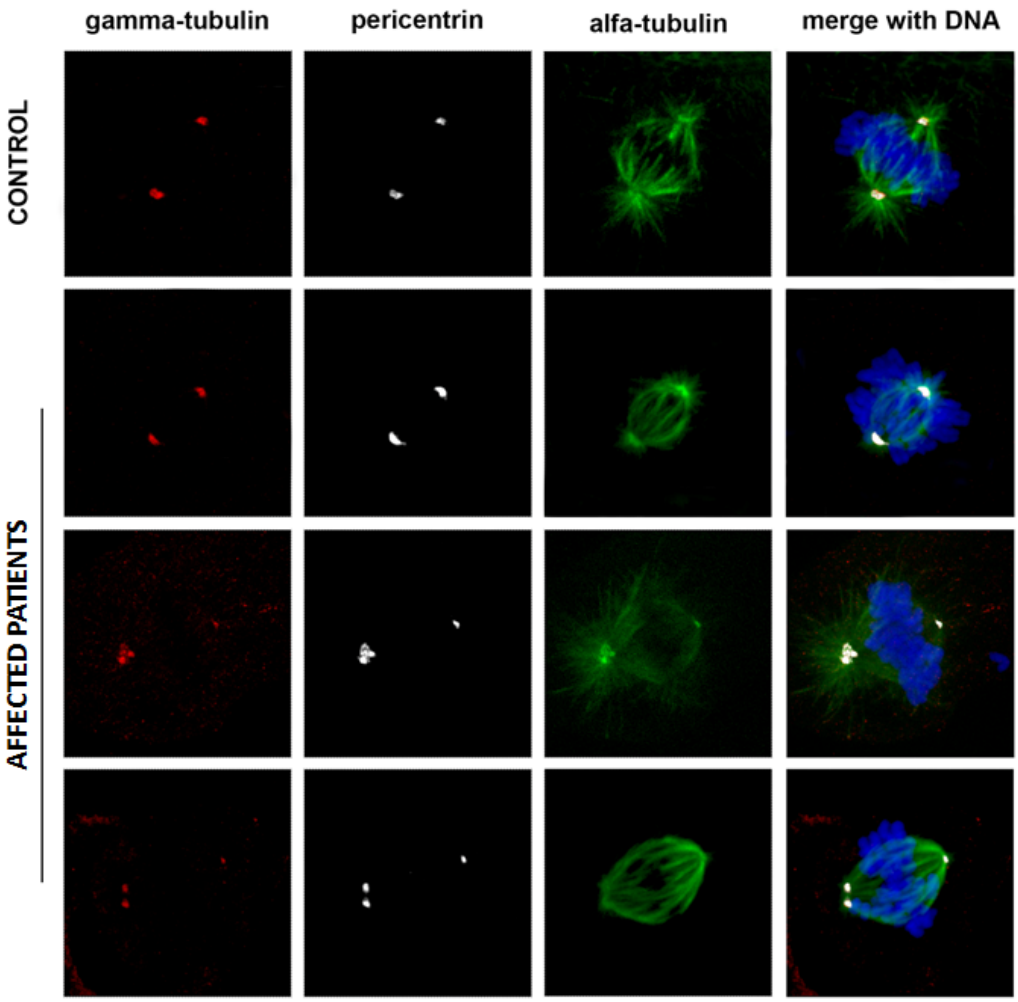

Figure S2. Confocal laser scanning microscopy (CLSM) observations of patient fibroblasts documenting an anomalous mitotic spindle organization.
CLSM analysis performed in synchronized skin fibroblasts from subjects with biallelic *TBCE* mutations show abnormal structures of the mitotic spindle during metaphase. Note the enhanced pericentrin signal, reduced aster formation, asymmetry of spindle and multispot of pericentrin and γ-tubulin compared to control cells. Fibroblasts were stained with pericentrin (grey), γ-tubulin (red), as centrosome markers, and α-tubulin (green) as a marker for microtubules and the mitotic spindle; chromosomes are DAPI stained (blue). Representative images obtained from fibroblasts of subjects 1544334 and 2518864 are shown. Scale bars, 5 μm.

Table S1. Whole exome sequencing data output.

	Family 1	Family 2	Family 3
Target regions coverage, 2x[1]	98.8%	98.7%	98.2%
Target regions coverage, 10x[1]	96.6%	97.2%	96.6%
Target regions coverage, 20x[1]	89.6%	93.7%	93.3%
Average sequencing depth on target[1]	56x	77x	110x
Number of variants with predicted functional effect	13,580	13,631	11,531
Novel, clinically associated, and unknown/low frequency variants[2]	346	346	237
Putative disease genes (autosomal recessive/X-linked trait)	12[3]	12[4]	5[5]
Shared candidate genes (autosomal recessive/X-linked trait)[6]	1, *TBCE*	1,*TBCE*	1, *TBCE*
Genes with putative *de novo* variants	2[7]	3[8]	5[9]
Shared genes with putative *de novo* variants[6]	-	-	-

[1]Referred to SureSelect Human All Exon V.4 (Families 1 and 2) and Agilent Clinical Research Exome (Family 3).

[2]MAF <0.1% in dbSNP144 and ExAC V. 0.3 databases, and with frequency <2% in our *in-house* database.

[3]*AR* (c.228_239dupGCAGCAGCAGCA, p.Gln77_Gln80dup), *ATXN1* (c.672_674dupGCA, p.Gln225dup), *CXorf21* (c.223C>A, p.His75Asn), *FUCA2* (c.-163C>T), *GFI1* (c.925-12_925-5delCTCTCTCT), *IGSF1* (c.877C>T, p.His293Tyr), *NBPF8* (c.1111G>T, p.Ala371Ser), *TBCE* (c.464T>A, p.Ile155Asn), *TRAK1* (c.2090_2095dupAGGAGG, p.Glu697_Glu698dup), *TRO* (c.2462C>T, p.Ala821Val), *ZBTB33* (c.740A>G, p.Gln247Arg), *ZNF469* (c.1409C>G, p.Pro470Arg; c.8701G>A, p.Glu2901Lys).

[4]*BCL2L11* (c.-208C>T), *CCDC150* (c.697T>G, p.Ser233Ala; c.3122G>A, p.Gly1041Asp), *FAM47B* (c.1687A>C, p.Ser563Arg), *GVQW2* (c.159-6delT), *NHS* (c.4127A>G, p.Gln1376Arg), *NOP9* (c.504_509dupGGAGGA, p.Glu168_Glu169dup), *PPP4R4* (c.2373T>G, p.Cys791Trp), RBMXL3 (c.1191_1192insAACGCCCACAGCGGAGGCCGCTCACCC, p.Pro397_Asp398insAsnAlaHisSerGlyGlyArgSerPro), *SPTB* (c.371A>G, p.Lys124Arg; c.964A>G, p.Ile322Val), *TBCE* (c.464T>A, p.Ile155Asn; c.1076delC, p.Ser360Ter), *USF3* (c.4404_4409dupGCAGCA, p.Gln1469_Gln1470dup), *ZDHHC11* (c.1059-8C>G).

[5]*BAHCC1* (c.1070C>T, p.Ala357Val; c.6838G>A, p.Gly2280Ser), *SEC14L5* (c.740T>C, p.Ile247Thr; c.1981_1984dupGGCT, p.Ser662fs), *ST8SIA2* (c.843-17_843-5dupTTTTTTTTTTTTT), *TBCE* (c.464T>A, p.Ile155Asn), *TTN* (c.42904G>A, p.Asp14302Asn; c.81038G>A, p.Arg27013Gln; c.91307G>A, p.Arg30436Gln)

[6]Filtering retained functionally relevant variants (excluding variants predicted as benign by CADD and metaSVM algorithms) in all affected subjects.

[7]*DCHS2* (c.7513G>A, p.Ala2505Thr); *DOCK2* (c.3375C>A, p.Phe1125Leu).

[8]*C17orf77* (c.653G>A, p.Arg218Lys), *HRCT1* (c.299_310dupTCCACCACCACC, p.Leu100_His103dup), *PTGES3L* (c.562-8G>C).

[9]*CARD10* (c.2864+7T>G); *CD40* (c.647-5_647-3dupTTT); *CNTNAP3B* (c.743-4dupT); *SERTAD4* (c.-17-8C>G); *TNN* (c.3760-6delT).

Table S2. Haplotype analysis of the genomic region flanking the c.464T>A change. Haplotypes referred to seven informative SNP/STR markers encompassing the *TBCE* gene documenting a 0.5 Mbp genomic region shared by all chromosomes carrying the c.464T>A change. Recombination was demonstrated at markers STR-1 and ST5-5, indicating that the genomic stretch defining the shared haplotype is < 1.0 Mbp. The haplotype referred to the chromosome bearing the c.1076delC in subject 2518864 is also shown (blue).

Marker/mutation[a]	Subjects									
	1544334		2518864[b]		VN X3359		VN X3360		00997847[c]	
STR-1 (chr1:234,859,467)	156	169	156	156	169	169	169	169	169	169
STR-2 (chr1:235,268,140)	360	360	360	366	360	360	360	360	360	360
D1S2649 (chr1:235,378,863)	431	431	431	442	431	431	431	431	431	431
rs780472451[d] (chr1:235,590,458)	A	A	A	T	A	A	A	A	A	A
rs750781063[e] (chr1:235,599,883)	C	C	C	-	C	C	C	C	C	C
STR-3 (chr1:235,638,265)	174	174	174	170	174	174	174	174	174	174
rs35346732 (chr1:235,715,532)	A	A	A	G	A	A	A	A	A	A
STR-4 (chr1:235,763,717)	316	316	316	324	316	316	316	316	316	316
STR-5 (chr1:235,829,526)	221	221	221	223	221	221	221	221	221	213

[a]Location is referred to hg19.

[b]This subject is compound heterozygote for the c.464T>A (p.Ile155Asn) and c.1076delC (p.Leu360Ter) changes.

[c]Haplotype shared with subject 00997844.

[d]c.464T>A (p.Ile155Asn), 0.0000082 (ExAC)

[e]c.1076delC (p.Leu360Ter), 0.00002 (ExAC)